Population genomics reveals molecular determinants of specialization to tomato in the polyphagous fungal pathogen Botrytis cinerea in France

Alex Mercier, Adeline Simon, Nicolas Lapalu, Tatiana E Giraud, Marc Bardin, Anne-Sophie Walker, Muriel Viaud, Pierre Gladieux

POPULATION GENOMICS REVEALS MOLECULAR DETERMINANTS OF SPECIALIZATION TO TOMATO IN THE POLYPHAGOUS FUNGAL PATHOGEN *BOTRYTIS CINEREA* IN FRANCE

Alex Mercier[1,2], Adeline Simon[1], Nicolas Lapalu[1], Tatiana Giraud[3], Marc Bardin[4], Anne-Sophie Walker[1†], Muriel Viaud[1†] and Pierre Gladieux[5*†]

[1] Université Paris-Saclay, INRAE, AgroParisTech, UMR BIOGER, 78850 Thiverval-Grignon, France

[2] Université Paris-Saclay, Orsay, France

[3] Ecologie Systématique Evolution, CNRS, Université Paris-Saclay, AgroParisTech, 91400 Orsay, France

[4] UR0407 Pathologie Végétale, INRAE, 84143 Montfavet, France

[5] PHIM Plant Health Institute, Univ Montpellier, INRAE, CIRAD, Institut Agro, IRD, Montpellier, France

[*] Corresponding author: pierre.gladieux@inrae.fr

[†] contributed equally to this study

Abstract

Many fungal plant pathogens encompass multiple populations specialized on different plant species. Understanding the factors underlying pathogen adaptation to their hosts is a major challenge of evolutionary microbiology, and it should help preventing the emergence of new specialized pathogens on novel hosts. Previous studies have shown that French populations of the grey mould pathogen *Botrytis cinerea* parasitizing tomato and grapevine are differentiated from each other, and have higher aggressiveness on their host-of-origin than on other hosts, indicating some degree of host specialization in this polyphagous pathogen. Here, we aimed at identifying the genomic features underlying the specialization of *B. cinerea* populations to tomato and grapevine. Based on whole genome sequences of 32 isolates, we confirmed the subdivision of *B. cinerea* pathogens into two genetic clusters on grapevine and another, single cluster on tomato. Levels of genetic variation in the different clusters were similar, suggesting that the tomato-specific cluster has not recently emerged following a bottleneck. Using genome scans for selective sweeps and divergent selection, tests of positive selection based on polymorphism and divergence at synonymous and non-synonymous sites and analyses of presence/absence variation, we identified several candidate genes that represent possible determinants of host specialization in the tomato-associated population. This work deepens our understanding of the genomic changes underlying the specialization of fungal pathogen populations.

Keywords: Host specialization; grey mould; gene content variation; selective sweeps; positive selection

Introduction

Many fungal plant pathogens encompass multiple lineages, host races or *formae speciales* specialized on different plant species. Understanding the proximate (*i.e.* molecular) and ultimate (*i.e.* eco-evolutionary) factors underlying adaptation to hosts is a major goal for evolutionary microbiology, because emerging diseases are often caused by the appearance and spread of new pathogen populations specialized onto new hosts (Fisher *et al.* 2012; Stukenbrock & McDonald 2008). Evolutionary theory predicts that pathogen specialization should facilitate the emergence of new populations onto novel hosts, because specialization restricts encounters of potential mates within hosts and reduces the survival of offspring due to maladaptation of immigrants and hybrid offspring, thereby reducing gene flow between ancestral and emerging populations (Giraud *et al.* 2010; Nosil *et al.* 2005). The role of specialization as a barrier to gene flow is expected to be strong for pathogens mating within or onto their hosts because, for individuals evolving the ability to infect novel hosts, mating automatically becomes assortative with respect to host use, and reproductive isolation arises as a direct consequence of adaptive divergence (Gladieux *et al.* 2011; Servedio *et al.* 2011). Evolutionary theory also predicts that specialization, and the associated emergence of new populations, could be facilitated by the molecular basis of plant-pathogen interactions, because compatibility is often determined by a limited number of genes in the host and the pathogen, and selection is more efficient when it acts on a smaller number of genes (Giraud *et al.* 2010; Schulze-Lefert & Panstruga 2011). However, despite the apparent ubiquity of specialized fungal pathogens and the negative impact that specialized populations can have on food security and ecosystem health, the genomic features involved in host specialization

remain largely unknown. Acquiring knowledge about the genomic features underlying pathogen specialization can provide key insights into the mechanisms of specialization.

The ascomycete *Botrytis cinerea* is often presented as a textbook example of a polyphagous plant pathogen, parasitizing more than 1400 host plant species belonging to 580 genera (Elad *et al.* 2016). Previous population genetic studies reveal that *B. cinerea* is not strictly speaking a generalist pathogen, and that a more appropriate qualifier is "polyspecialist", i.e. a set of populations specialized to different host species. Indeed, with the exception of California (Ma and Michailides, 2005; Caseys et al, 2020; Soltis et al, 2019; Atwell et al, 2015), studies conducted in multiple regions of the world reveal that populations were structured (reviewed in Walker 2016), and recognize the host as the factor with the highest explanatory power for population structure in *B. cinerea*, ahead of geography. In France, our previous work revealed population subdivision in *B. cinerea,* with genetic differentiation between field populations infecting tomato (*Solanum lycopersicum*) and grapevine (*Vitis vinifera*), respectively (Walker *et al.* 2015). This population structure in *B. cinerea* was shown to be stable in time and was observed in multiple regions in France. Furthermore, this structure was later associated with differences in performance on the two hosts, with pathogens isolated from tomato being more aggressive on tomato than pathogens isolated from grapevine, and reciprocally (Mercier *et al.* 2019). Altogether, these data were consistent with a certain degree of specialization of *B. cinerea* populations onto these two host plants.

Here, we aimed to identify the molecular basis of host specialization in the *B. cinerea* tomato- and grapevine-associated populations, by addressing the following questions: (1) Can we confirm the genetic subdivision between *B. cinerea* populations from tomato and

grapevine using genomic data, and what is the degree of divergence between them? (2) Can we identify genes with footprints of positive selection and/or divergent selection in the genomes of populations specialized to different hosts, and what are their predicted functions? (3) Is there variation in gene content between *B. cinerea* populations associated with tomato and grapevine? To address these questions, we used a set of *B. cinerea* isolates collected on tomato and grapevine in different regions of France. We Illumina-sequenced their genomes and identified single nucleotide polymorphisms by mapping sequencing reads against a high-quality reference genome (van Kan *et al.* 2017). Because some tests of selection can be biased by population subdivision, while other tests are based on patterns of population differentiation, we first analyzed the population structure of *B. cinerea* collected on tomato and grapevine. To detect genes potentially involved in the specialization of *B. cinerea* to tomato, we searched for signatures of positive selection, by scanning genomes in the tomato population for selective sweeps, and by estimating the direction and intensity of selection using McDonald-Kreitman tests on coding sequences. Furthermore, we investigated signatures of divergent selection using genomic differentiation between populations, and we characterized variations in the presence/absence of predicted genes between populations collected on tomato and grapevine using *de novo* genome assemblies, gene prediction, and orthology analysis.

Materials and methods

Sample collection

Botrytis cinerea samples were selected in a collection of isolates (i.e. single-spored mycelial colonies) originating from three regions of France (Champagne, Occitanie and Provence) and previously characterized using analyses of population structure based on microsatellite markers and pathogenicity tests (Walker *et al.* 2015; Mercier *et al.*, 2019). For each region and each host, we randomly selected three to nine isolates with high membership proportions (q>0.9) in the cluster matching their host of origin in a previous analysis of population structure based on microsatellite genotyping (Table 1; Mercier *et al.* 2019). Collection sites were 15 to 133 km apart within regions, and 204 to 722 km apart between regions (Supplementary Figure S1). The set of 32 isolates originated from the following hosts: (i) tomato (*Solanum lycopersicum*; fruits; 13 isolates), (ii) grapevine (*Vitis vinifera*; berries; 16 isolates), (iii) bramble (*Rubus fruticosus*; berries; two isolates) and (iv) hydrangea (*Hydrangea macrophylla*; flower buds; one isolate). Samples from tomato originated from plastic tunnels with sides opened (Occitanie region) or glasshouses (Provence and Champagne regions). Mycelia were cultured on malt-yeast-agar (MYA; 20 $g.L^{-1}$ malt extract, 5 $g.L^{-1}$ yeast extract, 15 $g.L^{-1}$ agar) at 23°C under continuous light until conidiation, and stored as conidial suspensions in glycerol 20% at -80°C until use.

Pathogenicity tests on tomato plants

Isolates of *B. cinerea* collected from tomato or grape were cultivated on MYA medium in a growth chamber (21°C, 14 hours light) for 14 days. Conidia were then washed with sterile distilled water. The conidial suspension was filtered through a 30 µm mesh sterile filter to

remove mycelium fragments. The conidial concentration was determined with a haemacytometer and adjusted to 10^6 spores/mL. Seeds of tomato var. Clodano (Syngenta) were sown in compost and transplanted after one week in individual pots. Plants were grown in a glasshouse for 6 to 8 weeks where they received a standard commercial nutrient solution once or twice a day, depending on needs. Plants had at least eight fully expanded leaves when inoculated with a conidial suspension. Each isolate was inoculated on five plants, from each of which two leaves were removed, leaving 5-10 mm petiole stubs on the stems. Each pruning wound was inoculated with 10 µl of conidial suspension at 10^6 conidia/mL. Inoculated plants were incubated in a growth chamber in conditions conducive to disease development (21°C, 16h-photoperiod, 162 $\mu mol.s^{-1}.m^{-2}$, relative humidity > 80%). Due to a growth chamber area that did not allow all the isolates to be tested at the same time, nine series of pathogenicity tests were conducted with 10-12 isolates each, together with the BC1 reference isolate collected in 1989 in a tomato glasshouse in Brittany (Decognet *et al.* 2009). For each isolate, two to four independent repetitions of the pathogenicity test were performed. Lesion sizes (in mm) were assessed daily between the 4^{th} and the 7^{th} day post-infection and the Area Under the Disease Progress Curve (AUDPC; (Simko & Piepho 2012) was computed to take into account the kinetics of disease development for each isolate. To compare the aggressiveness of isolates, an aggressiveness index (AI), relative to the reference isolate BC1, was computed as follows: $AI_{isolate} = 100 \times (AUDPC_{isolate}/AUDPC_{BC1})$, where $AUDPC_{isolate}$ was the average AUDPC for a given isolate and $AUDPC_{BC1}$ is the average AUDPC for the reference isolate BC1. Using the AI index calibrating the AUDPC of a given isolate with that of the reference isolate BC1 in the same test allows comparing isolates aggressiveness while taking into account the variability

147 occurring among assays (e.g. plant physiological state; (Leyronas *et al.* 2018). Because of
148 data non-normality, data were analysed using non-parametric tests. Three statistical tests
149 were carried out with STATISTICA: (1) we used a non-parametric analysis of variance (Kruskal-
150 Wallis test) to assess differences among isolates in terms of aggressiveness on grape and
151 tomato, considering the average values for each of the independent pathogenicity tests as
152 replications; (2) we used the Mann-Whitney U-test to compare the aggressiveness of isolates
153 from different hosts of origin (tomato vs. grape), considering the independent repetitions of
154 the pathogenicity test as blocks and the 13 isolates from tomato and 16 isolates from
155 grapevine as replicates; (3) we used a Kruskal-Wallis test to compare isolates from three
156 different clusters (see *Results* section) in terms of aggressiveness on tomato plants.
157

158 *DNA preparation and sequencing*

159 Isolates were cultivated for 48 h on MYA + cellophane medium at 23 °C in the dark and then
160 ground using a mortar and pestle in liquid nitrogen. DNA was extracted using a standard
161 sarkosyl procedure (Dellaporta *et al.* 1983). Paired-end libraries were prepared and
162 sequenced (2 x 100 nucleotides) on a HiSeq4000 Illumina platform at Integragen (Evry,
163 France). Sequencing coverage ranged from 58 to 305 X. Genomic data were deposited at SRA
164 under accession number PRJNA624742. Read quality was checked using FASTQC
165 (https://www.bioinformatics.babraham.ac.uk/projects/fastqc/).
166

SNP calling and filtering

SNPs were detected with the same workflow as described in (Zhong *et al.* 2017). Sequencing reads were preprocessed with TRIMMOMATIC v0.36 (Bolger *et al.* 2014). Preprocessed reads were mapped onto the *B. cinerea* B05.10 reference genome (van Kan *et al.* 2017) using BWA v0.7.15 (Li & Durbin 2009). Aligned reads were filtered based on quality using SAMTOOLS v1.3 (Li *et al.* 2009) and PICARD TOOLS (http://broadinstitute.github.io/picard/) to remove secondary alignments, reads with a mapping quality <30 and paired reads not at the expected distance. SNP calling was performed with FREEBAYES v1.1 (Garrison & Marth 2012). Further filtering was carried out using script VCFFiltering.py (https://urgi.versailles.inra.fr/download/gandalf/VCFtools-1.2.tar.gz), following (Li 2014). We kept only biallelic SNPs supported by more than 90% of aligned reads, detected outside low-complexity regions or transposable elements (as identified in the reference isolate B05.10: https://doi.org/10.15454/TFYH9N; Porquier *et al.* 2016) and with coverage lower than twice the standard deviation from the mean depth coverage. The VCF file is available on Zenodo (doi: 10.5281/zenodo.4293375).

Population structure and demographic history

We performed a principal component analysis based on biallelic SNPs using the python library SCIKIT-ALLEL 1.3.2 (https://github.com/cggh/scikit-allel). We used the sNMF program to infer individual ancestry coefficients in *K* ancestral populations. This program is optimized for the analysis of large datasets and it estimates individual admixture coefficients based on sparse non-negative matrix factorization, without assuming Hardy-Weinberg equilibrium (Frichot et al., 2014). We used SPLITSTREE 4 (Huson & Bryant 2005) to visualize relationships

between genotypes in a phylogenetic network, with reticulations representing the conflicting phylogenetic signals caused by recombination or incomplete lineage sorting. The position of the root was determined using a *B. fabae* isolate as the outgroup. *Botrytis fabae* is one of the closest known relatives of *B. cinerea* (Amselem *et al.* 2011; Walker 2016). Summary statistics of genomic variation (segregating sites S, nucleotide diversity π, Watterson's θ, Tajima's D) were estimated using EGGLIB 3.0 (https://egglib.org/) on 10kb windows, excluding sites with more than 50% missing data and removing windows with lseff<1000 (lseff is the number of analysed sites) or nseff<3 (nseff is the average number of exploitable samples). Site frequency spectra were estimated using DADI 1.7.0 (GUTENKUNST *ET AL.* 2009). Allelic richness and private allele richness were estimated with ADZE 1.0 (Szpiech *et al.* 2008), using a generalized rarefaction approach to account for differences in sample size among populations.

We employed the f3 statistic (Reich *et al.* 2009) to test for admixture based on shared genetic drift, as implemented in the POPSTATS python script (Skoglund *et al.* 2015; https://github.com/pontussk/popstats/). The *f3* statistic is used to test for admixture among three populations Px, P1, P2. In the no-admixture case, the *f3* statistic measures the branch length between Px and the internal node of the unrooted population tree (Px;P1,P2), and it is therefore expected to be greater than zero. In the case Px has a mixed ancestry from P1 and P2, or populations closely related to them, the *f3* statistic is expected to be negative. Significance was assessed by block jackknife by treating each chromosome as a block and weighting each block by the number of SNPs. The standard error of the test statistic was used to define a Z-score.

212

213 *Genome assembly and gene prediction*

214 Gene content was determined using two independent approaches. In the first approach,
215 we used the read mapping coverage of the genes previously predicted in the reference
216 genome B05.10 (van Kan *et al.* 2017). Read count per site for each gene and for each isolate
217 was computed using SAMTOOLS BEDCOV, and normalized using EDGER (McCarthy *et al.* 2012;
218 Robinson *et al.* 2010). Genes showing significant differences in mapping coverage across
219 populations were identified with EDGER (adjusted p-value <0.05 and more than two-fold
220 change). Putative gene duplication events (higher mapping coverage) and missing B05.10
221 genes (lack of mapping reads) were visually inspected in their genomic context using a
222 genome browser for validation.

223 The second approach was based on genome assembly and *de novo* gene prediction.
224 Illumina paired-reads were assembled using a combination of VELVET (Zerbino & Birney
225 2008), SOAPDENOVO and SOAPGAPCLOSER (Luo *et al.* 2012), as follows: (1) reads were trimmed
226 at the first N, (2) contigs were generated with several k-mer values using SOAPDENOVO, (3)
227 several VELVET assemblies were built using several k-mer values and as the input the trimmed
228 reads and all SOAPDENOVO contigs considered as "long reads ", (4) the assembly that
229 maximizes the criterion (N50*size of the assembly) was selected, (5) SOAPGAPCLOSER was run
230 on the selected assembly, and (6) Contigs completely included in other longer contigs were
231 deleted. Genomic regions mapping to transposable elements previously identified in *B.*
232 *cinerea* (https://doi.org/10.15454/TFYH9N; Porquier *et al.* 2016) were masked with
233 REPEATMASKER (http://www.repeatmasker.org) prior to gene prediction. Genes were
234 predicted using the FGENESH *ab initio* gene-finder (Solovyev *et al.* 2006;

http://www.softberry.com/berry.phtml), the program previously used to annotate the reference genome (Amselem *et al.* 2011), and for which *Botrytis*-specific gene-finding parameters were thus available. Completeness of the assembly and gene prediction were evaluated with BUSCO using the Ascomycota gene set (Seppey *et al.* 2019). We then used ORTHOFINDER (Emms & Kelly 2015) in order to define groups of orthologous sequences (hereafter "groups of orthologs") based on sequences of predicted genes translated into protein sequences. To reduce the impact of incomplete gene prediction (*e.g.* truncated genes in small contigs), groups of orthologs were then manually checked for the presence/absence of the protein-encoding genes in the genomes using TBLASTN (Johnson *et al.* 2008). Proteins were functionally annotated using INTERPROSCAN (Jones *et al.* 2014), and SIGNALP (Almagro Armenteros *et al.* 2019) was used to predict secretion signal peptides. Prediction of transmembrane helices in proteins was performed using TMHMM 2.0 (Krogh *et al.* 2001; Sonnhammer *et al.*). As we detected traces of bacterial contamination in the genome of the Sl13 isolate, this genome was not included in orthology analysis. However, we have kept this genome for analyzes based on polymorphism, because bacterial reads cannot map to the reference genome.

Tests of positive selection based on polymorphism and divergence at synonymous and non-synonymous sites

We estimated the intensity and direction of selective pressures exerted on genes in populations using the McDonald-Kreitman test based on polymorphism and divergence at synonymous and non-synonymous sites (McDonald & Kreitman 1991). This test is based on the number of nucleotide polymorphisms and substitutions in gene sequences, and assumes

that synonymous mutations are neutral. Pseudo-sequences for coding sequences of all genes in the reference genome were generated using the VCF file and the reference sequence. Synonymous and non-synonymous divergence was computed with CODEML (model 0; Yang 1997, 2007), using *B. fabae* as the outgroup. Synonymous and non-synonymous polymorphism was computed using EGGLIB 3 (https://egglib.org/), filtering out sites with more than 80% missing data and excluding filtered alignments with less than 10 codons or four sequences. Samples Sl1, Sl2, Sl3, Sl13, Vv3, Vv5, Vv2, Vv4 and Vv6 were excluded because they introduced missing data that prevented calculations of synonymous and non-synonymous divergence. The neutrality index (NI), defined as $(P_N/D_N)/(P_S/D_S)$ (Stoletzki & Eyre-Walker 2011), was computed for every gene, with P_N and D_N the numbers of non-synonymous polymorphisms and substitutions, respectively, and P_S and D_S the numbers of synonymous polymorphisms and substitutions, respectively. Pseudocounts of one were added to each cell of the McDonald-Kreitman tables to ensure the NI was always defined (*i.e.* no division by zero).

Linkage disequilibrium and recombination

We used POPLDDECAY (Zhang *et al.* 2019a) to measure linkage disequilibrium (r^2) as a function of the distance between pairs of SNPs. POPLDDECAY was configured with a maximum distance between SNPs of 300 kbp, a minor allele frequency of 0.005 and a maximum ratio of heterozygous allele of 0.88. Recombination rates were estimated for each chromosome with PAIRWISE in LDHAT version 2.2 (Auton & McVean 2007). Sites with missing data were excluded.

Tests of positive selection based on linkage disequilibrium and the site frequency spectrum

We searched for signatures of selective sweeps along genomes using three different softwares, each implementing a different approach. The SWEED 3.0 software (Pavlidis *et al.* 2013) implements a composite likelihood ratio (*CLR*) test based on the SWEEPFINDER algorithm (Nielsen *et al.* 2005), which uses the site frequency spectrum (SFS) of a locus to compute the ratio of the likelihood of a hard selective sweep at a given position to the likelihood of a null model hypothesis without selection. The CLR statistic was computed for each chromosomes of each population using a grid size of 50 or 200 (grid size is the number of positions where the likelihood is calculated), but only results for a grid size of 200 are presented because the CLR profiles were highly similar between the two settings. Input files included both "unfolded" SNPs (i.e. SNPs for which ancestral and derived states can be determined using the allelic state of the outgroup) and "folded" SNPs (i.e. SNPs for which the outgroup had missing data). Only biallelic sites with sample size greater than or equal to five were included. The nS_L method implemented in the NSL software (Ferrer-Admetlla *et al.* 2014) detects hard and soft selective sweeps based on haplotype homozygosity. The nSL statistic was computed for each chromosome of each population, including only biallelic sites with sample size greater than or equal to five. Nine isolates (Sl1, Sl2, Sl3, Sl13, Vv3, Vv5, Vv2, Vv4, Vv6) were excluded to reduce the proportion of missing data. The *hapFLK* method (Fariello *et al.* 2013) implemented in the HAPFLK software is based on the original *FLK* method by (Bonhomme *et al.* 2010), which detects signatures of selection from differentiation between populations. This metric was used to test the null hypothesis of neutrality by contrasting allele frequencies at a given locus in different populations. *hapFLK* extends the FLK method to account for the haplotype structure in the sample, and the method is robust to the effects of bottlenecks and migration. HAPFLK takes the number of cluster of haplotypes as a

parameter (K). To determine the number of clusters of haplotypes K, we ran FASTPHASE v1.4 (Scheet & Stephens 2006) and R package IMPUTEQ (Khvorykh & Khrunin 2020) on polymorphism data for the largest chromosome BCIN01. For each population, we used IMPUTEQ to generate five datasets with 10% of polymorphic positions masked, and for each masked dataset we used FASTPHASE for imputing masked positions assuming clusters of K=2,3...10 haplotypes and the following parameters: -T10 -C25 -H-1 -n -Z. We estimated error using Estimate-Errors function in IMPUTEQ and the number of clusters that minimizes the error was selected as the optimum. The HapFLK metric was computed individually on each chromosome using as number of clusters K = 5, and nfit = 2. Accessory chromosomes were not included in these analyses as they showed presence/absence polymorphism (see *Results* section).

Results

Whole-genome sequencing, population structure and demographic history

Previous work using microsatellite data revealed differentiation between populations of *B. cinerea* collected on tomato and grapevine (Mercier *et al.* 2019; Walker *et al.* 2015). To investigate the genetic basis of specialization of the tomato- and grapevine-infecting populations, we randomly selected for genome sequencing 32 isolates collected on tomato (13 isolates), grapevine (16 isolates), *Rubus* (two isolates) and *Hydrangea* (one isolate) (Table 1). Isolates from *Rubus* and *Hydrangea* were previously shown to belong to generalist populations (*i.e.* assigned to clusters found on all sampled hosts; Mercier *et al.* 2019). One isolate of the sister species *B. fabae* was also sequenced and used as the outgroup. Information about the sequenced isolates is summarized in Table 1. Alignment of sequencing

reads to the B05.10 reference genome (van Kan *et al.* 2017) followed by SNP calling identified 249,084 high-quality SNPs.

In clustering analyses based on sparse nonnegative matrix factorization algorithms, as implemented in the sNMF program (Frichot et al., 2014), the model with *K*=4 clusters was identified as the best model based on cross-entropy (Supplementary Figure S2) and models with K>4 did not identify well-delimited and biologically relevant clusters (Fig. 1A). At K=4, one cluster was associated with tomato (hereafter referred to as "T" cluster), two clusters were associated with grapevine (hereafter referred to as "G1" for the largest, and "G2" for the smallest), and one cluster was formed by the isolates Rf1 and Hm1 from bramble (*R. fruticosus*) and hydrangea (*H. macrophylla*) (Figure 1A). The isolate Rf2 collected on wild blackberry displayed ancestry in multiple clusters, and the reference isolate B05.10 had ancestry in the G2 and T clusters. No pattern of geographical subdivision was observed, consistent with previous findings (Walker *et al.* 2015; Mercier *et al.,* 2019). The neighbor-net network inferred with SPLITSTREE revealed three main groups, corresponding to the three main clusters identified with sNMF, with cluster G2 (isolates Vv8, Vv9, Vv11 and Vv15) more closely related to T than to G1 (Figure 1B). Reticulations in the neighbor-net network and patterns of membership at K=2 and K=3 in the analysis with sNMF indicated that cluster G2 shared recent ancestry with clusters G1 and T. However, tests for admixture using the f3 statistic (Reich *et al.* 2009; Skoglund *et al.* 2015) did not support a scenario in which G2 derived from admixture between the two other clusters (Supplementary Table S1). The principal component analysis corroborated the results of clustering analyses and the neighbor-net network (Figure 1C). The first principal component separated isolates Hm1 and Rf1 from the rest of the dataset. The second principal component individualized isolate Rf2,

as well as the three clusters T, G1 and G2. The third and fourth principal components individualized cluster G2 and isolate Sl11, respectively. Together, analyses of population subdivision revealed three clearly defined populations (two on grapevine and one on tomato) and we therefore focused on these populations to identify the genes underlying differences in host specialization.

On average across core chromosomes BCIN01 to BCIN16, nucleotide diversity π and Watterson's θ were comparable in the three populations (from π=0.0018/bp in G1 to π =0.0030/bp in G2; from θ=0.0017/bp in G1 to θ=0.0027/bp in G2; Table 2; Supplementary Table S2), although all comparisons were statistically significant except between populations T and G2 for θ (two-tailed Wilcoxon signed-rank test, P-value>0.05). Allelic richness was slightly higher in G2 than in T (AR=1.104 vs AR=1.094), and lower in G1 (AR=1.078). Private allele richness was higher in G1 (PAR=0.085), than in T (PAR=0.073) and G2 (PAR=0.071) (Table 2).

The site frequency spectra estimated in populations G1 and T were U-shaped, indicating an excess of high-frequency derived alleles (Figure 2; population G2 was excluded because of too small a sample size), consistent with ongoing episodes of positive selection, mis-assignment of ancestral alleles or gene flow (Marchi & Excoffier 2020). Estimates of Tajima's D were positive but close to zero in clusters T and G1 (T: D=0.309; G1: D=0.167), indicating a slight deficit of low frequency variants (Table 2; Supplementary Table 2), consistent with balancing selection or population contraction. In cluster G2, the estimated Tajima's D was D=1.470 but the estimate was likely upwardly biased by the small sample size, because Watterson's θ is underestimated when sample size is small. The distance at which linkage disequilibrium (LD) decayed to 50% of its maximum was an order of magnitude longer in G2

372 (LDdecay50: 16,800bp) than in T (LDdecay50: 8600bp) and G1 (LDdecay50: 3100bp)
373 (Supplementary Figure S3). The recombination rate was higher in G2 (ρ=0.2047/bp) than in
374 G1 and T (G1: ρ=0.0178/bp; T: ρ=0.0108/bp).

375 The accessory chromosome BCIN18 showed no polymorphism in all three population and
376 the accessory chromosome BCIN17 showed no polymorphism in population G2
377 (Supplementary Table S2). However, it should be noted that coverage analysis also revealed
378 that these accessory chromosomes, which contain a reduced number of genes (23 and 19
379 respectively, van Kan *et al.* 2017), were distributed irrespectively of the host of origin:
380 BCIN17 was found present in all but three isolates (Sl9, Sl10 and Vv15), while BCIN18 was
381 only present in five isolates (Sl3, Sl5, Sl9, Vv9 and Vv11; Supplementary Table S3). In
382 population T, the accessory chromosome BCIN17 displayed a relatively high and positive
383 value of Tajima's D (D=1.37; Supplementary Table S2) and approximately twice as much
384 nucleotide diversity as in core chromosomes (π=0.0058/bp; Supplementary Table S2). In
385 population G1, accessory chromosome BCIN17 displayed a negative value of Tajima's D (D=-
386 0.845) and two orders of magnitude less nucleotide diversity than core chromosomes
387 (π=5.7e-5/bp; Supplementary Table S2). The differences in Tajima's D estimates for BCIN17
388 reflect the existence of two divergent haplotypes in T, but not in G1 (not shown).
389

390 *Isolates from the T population are more aggressive on tomato plants.*

391 To test whether isolates collected on tomato are more aggressive on their host of origin,
392 compared to isolates collected on grapevine, pathogenicity assays were performed on whole
393 tomato plants in controlled conditions. To assess differences among isolates in terms of
394 aggressiveness on grape and tomato, we used a non-parametric analysis of variance,

395 considering the average values for each of the independent pathogenicity tests as
396 replications. We found a significant isolate effect (Kruskal Wallis test, H (28, N= 87)
397 =69.89221, $p < 0.0001$), consistent with the wide range of aggressiveness levels observed for
398 the 29 isolates.

399 To compare the aggressiveness on tomato of isolates from different hosts of origin
400 (tomato vs. grape), we tested for differences in the distribution of the aggressiveness index
401 between isolates originating from the two types of hosts, considering the independent
402 repetitions of the pathogenicity test as blocks and the 13 isolates from tomato and 16
403 isolates from grapevine as replicates. We observed a significant effect of the host of origin
404 (Figure 3, Mann-Whitney U test, $p < 0.0001$) and T isolates collected on tomato were on
405 average 2.7 times more aggressive on tomato plants than isolates collected on grapevine.

406 To compare the aggressiveness on tomato of isolates from three different clusters (T, 13
407 isolates; G1, 12 isolates; G2, 4 isolates), we tested whether the aggressiveness index of
408 isolates from different clusters originate from the same distribution. A Kruskall-Wallis test
409 rejected the null hypothesis that all clusters display the same median of the aggressiveness
410 index (H (2, N= 87) =19.80083, $p < 0.0001$). The T population was significantly different from
411 the G1 population but not from G2 (Kruskall-Wallis test, $p< 0.0001$ and $p = 0.37$,
412 respectively). G2 and G1 were not significantly different (Kruskall-Wallis test, $p = 0.57$).

413

414 *Gene content slightly differs between tomato- and grapevine-associated populations*

415 As variation in gene content can be involved in adaptation to novel hosts (Cummings *et al.*
416 2004; Inoue *et al.* 2017; Langridge *et al.* 2015), we sought to identify genes specific to the
417 tomato (T) and grapevine (G1 and G2) populations. We first explored the mapping coverage

of genes previously identified in the B05.10 reference to identify sets of genes that were missing or showing duplication events (Supplementary Table S4). Five B05.10 genes were identified as missing in the T population, including four consecutive genes in the subtelomeric region of chromosome BCIN02 that could correspond to a secondary metabolism gene cluster. Among these four genes, one is coding for a NRPS-like enzyme similar to the protein MelA of *Aspergillus terreus* involved in the biosynthesis of an α-keto acid dimer (Geib et al. 2016), two other genes encode putative biosynthetic enzymes (FAD-binding and enoyl reductase domains). Mapping coverage of B05.10 genes also suggested some possible duplication events in a subtelomeric region of chromosome BCIN08, with T isolates showing approximately three times as many reads as the G1 and G2 isolates for the four consecutive genes Bcin08g00060 to Bcin08g00090. This suggested that the corresponding region of at least 25 kb would be in three copies in the genomes of the T isolates. Among the four duplicated genes, two encode carbohydrate-active enzymes (CAZymes) known as plant cell wall degrading enzymes (PCWDEs) as they act on pectin (glycoside hydrolase GH28) and hemicellulose or pectin side chains (GH43).

We also analysed the variation in gene content using a different approach that makes no use of reference genome B05.10. We built *de novo* assemblies of the genomes of T, G1 and G2 isolates. The genome assembly size of the 28 isolates ranged from 41 Mb to 42.5 Mb (Supplementary Table S5), which was slightly smaller than the genome assembly size of the B05.10 reference isolate (42.6 Mb). We then predicted genes *ab initio* using FGENESH. The number of predicted genes ranged from 11,109 to 11,311 among genomes. To compare gene content in the T, G1 and G2 populations, we used ORTHOFINDER to identify 12,319 groups of orthologous sequences (i.e., orthogroups). The number of groups of orthogroups

441 shared by pairs of isolates within populations was higher that between populations
442 (Supplementary Table S6). By looking for orthologous groups that were present in at least
443 75% of the genomes of a focal population and missing in other populations, we identified 21
444 G1-specific genes, a single G2-specific gene, five genes specific to the G1 and G2 populations
445 (those already detected with the first approach described above), two genes missing
446 specifically in the G1 population, and a single gene specific to the T population
447 (Supplementary Table S7). This latter gene was a GH71 glycoside hydrolase (OG0011490, an
448 α-1,3-glucanase; (Lombard *et al.* 2014) acting on fungal cell wall. Among the genes specific
449 to G1, we found a GH10 glycoside hydrolase (in OG0011469; (Lombard *et al.* 2014) acting on
450 plant cell wall (*i.e.* hemicellulose). The proteins encoded by the other G1-specific genes had
451 no functional prediction though four of them shared a domain typical of metalloenzymes
452 (IPR11249) with putative peptidase activities and three other ones showed a versatile
453 protein-protein interaction motif involved in many functions (IPR011333). Two proteins with
454 secretion signal peptides were also found specific to G1 (OG0011305 and OG0011366), with
455 OG0011366 having a predicted function of interferon alpha-inducible protein-like (Rosebeck
456 & Leaman 2008) and a predicted transmembrane helix.

457 Together, these analyses revealed that the magnitude of gene content variation is limited
458 between *B. cinerea* populations, which emphasizes the need to investigate differences in
459 allelic content at shared genes for elucidating the genomic basis of host specialization.

460

461 *McDonald-Kreitman tests of positive selection identify genes related to virulence*

462 We investigated differences in the direction and intensity of natural selection driving the
463 evolution of gene sequences in the two populations with the greatest difference in terms of

quantitative pathogenicity on grape and tomato, which are also the two populations with the largest sample size (G1 and T). More specifically, we searched for genes with signatures of positive selection in both populations that also show high sequence divergence between populations, or genes with signatures of positive selection in one population, but not in the other population. The direction and intensity of selection was estimated using neutrality indexes computed for each individual gene in each population based on McDonald-Kreitman tables of polymorphisms and substitutions at synonymous and non-synonymous sites, using *B. fabae* as the outgroup. The neutrality index is expected to be below one for genes under positive selection (due to an excess of non-synonymous substitutions) and above one for genes under negative selection (due to a deficit of non-synonymous polymorphisms). To identify genes potentially involved in host specialization, we first selected genes showing low values of the neutrality index in both populations (log [neutrality index] ≤-0.5), and high values of the inter-population dN/dS ratio (dN/dS in the top 5% percentile; Supplementary Figure S4). This analysis identified five genes: Bcin02p04900, Bcin07p02650, Bcin09p06530, Bcin14p01690, Bcin09p02190 (Supplementary Table S8). Two genes (Bcin07p02650, Bcin14p01690) code for glycosyl hydrolases of the GH5 family, a family that includes enzymes acting on plant cell walls and enzymes act on fungal cell walls. One of the two genes (Bcin14p01690), has a cellulose binding domain which strongly suggests a role as PCWDE. Two genes (Bcin02p04900, Bcin09p02190) are involved in basic cell functions (a DNA nuclease and a protein involved in ribosome biogenesis). The last gene (Bcin09p06530) has no known domain.

We also selected genes showing low values of the neutrality index in one population (log [neutrality index] ≤-0.5), and high values in the other (log [neutrality index]>=0)

(Supplementary Figure S4). This analysis identified 392 genes in G1 and 428 genes in T (Supplementary Table S8). Functional enrichment analyses revealed contrasting results in the G1 and T populations (Supplementary Table S8). In the G1 population, we identified a significant two-fold enrichment in transporter-encoding genes among the 392 genes with signatures of positive selection. These 28 transporters included many candidates with putative roles in nutrition such as the transport of sugars and amino-acids (five genes of each). Fifteen of them were proteins of the major facilitator superfamily (MFS). The MFS transporter-encoding genes included five putative sugar transporters and ten unknown transporters that could have roles in various processes, including obtaining nutrients from the host, efflux of fungi-toxic compounds or the export of fungal phytotoxins (Hartmann *et al.* 2018; Maruthachalam *et al.* 2011; Perlin *et al.* 2014). Finally, five of the 392 genes encoded ATPase transporters including the BcPrm1 P-type Ca2+/Mn2+-ATPase that mediates cell-wall integrity and virulence in *B. cinerea* (Plaza *et al.* 2015).

In the T population, the list of 428 genes with signatures of positive selection showed a significant 2.5-fold enrichment in genes encoding for proteins involved in oxidative stress response (eight genes). These genes encode enzymes that are able to detoxify reactive oxygen species *i.e.* glutathione-S-transferases (BcGST1, 9 and 24), the superoxide dismutase BcSOD1, and two peroxidases (BcPRX8 and BcCCP1). In addition, the list of 428 genes also included *BcatrO*, which encodes the transporter BcAtrO involved in the resistance to H_2O_2 (Pane *et al.* 2008).

A 2.5-fold enrichment was also observed for the genes coding for CAZYmes acting as PCWDEs (ten genes) especially for those involved in the modification of hemicellulose (five

509 genes; Espino *et al.* 2010 ; Supplementary Table S8) such as the xylanase BcXyn11A that is
510 required for full virulence on tomato (Brito *et al.* 2006).
511
512 *Selective sweeps in regions encompassing genes encoding enzymes involved in carbohydrates*
513 *metabolism*
514 To identify genomic regions with signatures of selective sweeps, we conducted three
515 different genome scans, using different features of the data: i) hapFLK, which detects hard
516 and soft sweeps based on patterns of differentiation between clusters of haplotypes
517 between populations; ii) nS_L, which detects hard and soft sweeps based on the distribution
518 of fragment length between mutations and the distribution of the number of segregating
519 sites between pairs of chromosomes; iii) and SweeD's CLR, which detects hard sweeps based
520 on the site frequency spectrum. The *CLR* and nS_L metrics are population-specific and were
521 computed for each population independently, while the *hapFLK* metric is F_{ST}-based and was
522 thus computed for populations G1 and T (Supplementary figure S5). We identified candidate
523 SNPs located in (hard or soft) selective sweeps as the SNPs that were in the top 5% of the
524 hapFLK statistic, but also in the top 5% of either the nSL or CLR statistic in a least one
525 population (Figure 4). In total, this approach identified 4,667 SNPs of which 1,300 were
526 localized in coding sequences, 256 in introns, 830 in untranslated transcribed regions, and
527 465 less than 1500bp upstream of coding sequences. These 2,851 SNPs corresponded to 351
528 genes, of which 15 were identified by SNPs in the top 5% of selective sweep metrics in both
529 populations, 200 by SNPs in the top 5% of selective sweep metrics in population T, and 175
530 by SNPs in the top 5% of selective sweep metrics in population G1 (Supplementary table S9).

Candidate genes in the selective sweep regions of each population included genes coding for proteins with functions consistent with a role in infection, such as transporters, CAZymes, putative effectors and two genes that are confirmed virulence factors. Indeed, one region identified in the G1 population contains the gene encoding the Pectin Methyl Esterase BcPme1 required for full virulence of *B. cinerea* on several host including grapevine (Valette-Collet *et al.* 2003), and another region contains the gene encoding BcCgf1, a small secreted protein that is essential for infection structure development (Zhang *et al.* 2020). Nevertheless, it is unlikely that all genes in selective sweep regions have been direct targets of positive selection, most of them being possible hitch-hikers. This could be the reason why no significant functional enrichment was detected among these genes.

Finally, comparison of the lists of genes identified in the selective sweep regions and those with signatures of positive selection according to McDonald-Kreitman tests identified nine genes in common for the T population and four genes in common for the G1 population (Supplementary table S9). This suggests that these genes were subjected to both recurrent positive selection for amino-acid changes and to recent positive selection in populations of *B. cinerea*. In addition, we can hypothesize that these genes may be the actual targets of positive selection, and that surrounding candidate genes could be only hitch-hikers. Functional annotations of the genes that show both recurrent positive selection for amino-acid changes and recent positive selection signals further indicated a cutinase-encoding gene (Bcin01g09430) in the T population and a sugar transporter encoding gene (Bcin16g00530) in the G1 population, and also pointed out various other functions.

Discussion

Genetic differentiation in B. cinerea *between populations associated with grapevine and tomato*

Genetic structure associated with the host of origin in *B. cinerea* has been extensively investigated (reviewed in Walker 2016). Most of the studies based on sufficient sampling size (n>100) found significant population differentiation between populations of *B. cinerea* from different hosts (e.g. in Chile, Tunisia, Hungary, United Kingdom; Walker 2016). One noticeable case is the population of *B. cinerea* collected from various hosts in California (Ma & Michailides 2005), for which whole-genome sequencing data did not detect any host-associated population structure despite differences in pathogenicity against different hosts (including tomato) in cross-infectivity assays (Atwell *et al.* 2015; Caseys *et al.* 2020; Soltis *et al.* 2019). In France, previous research concluded that *B. cinerea* populations were differentiated according to some of their hosts, including tomato, grapevine and, to a lesser extent, bramble (Fournier & Giraud 2008; Walker *et al.* 2015). In two recent studies comparing the aggressiveness of isolates coming from diverse hosts, the disease severity caused by isolates from tomato was significantly greater than the severity caused by isolates from grape or other crops, thus indicating that *B. cinerea* populations parasitizing tomato were specialized to this host (Bardin *et al.* 2018; Mercier *et al.* 2019). Here we show that populations parasitizing tomato and grapevine are subdivided into three populations, two being associated with grapevine (G1 and G2) and one with tomato (T). This pattern of population genetic structure differs from previous findings (Walker et al., 2015), as three populations parasitizing grapevine had previously been detected, but studies differ in terms of sampling and genotyping schemes (thousands of SNPs vs 8 SSR markers, and an order of

magnitude of difference in the size of sample sets). The clear pattern of population subdivision found in our study also stands in sharp contrast with the lack of host- or geography-associated population subdivision across various hosts, including tomato and grape, in California (Atwell *et al.* 2015; Atwell *et al.* 2018). This difference in population structure between France and California indicates that the factors leading to host-specific differentiation between *B. cinerea* pathogens from grape and tomato do not operate everywhere. The differences in LD decay (up to an order of magnitude longer in our study compared to Californian *B. cinerea*) and nucleotide diversity (half as much in our study compared to Californian *B. cinerea*) also suggest that the demographic history and population biology of the pathogen is contrasted between the two regions.

Multiple factors can contribute to reduce gene flow between populations parasitizing grapevine and tomato. A first possible factor limiting gene flow is adaptation to host. Mating in *B. cinerea* occurs on the host after infection, between individuals that were thus sufficiently adapted to infect the same host, which induces assortative mating with respect to host use and reduce opportunities for inter-population crosses (Giraud 2006; Giraud *et al.* 2010; Giraud *et al.* 2008). Another factor possibly limiting gene flow between populations infecting tomato and grape is habitat isolation (*i.e.* reduced encounters caused by mating in different habitats). Tomatoes are grown in nurseries before being dispatched to the fields, tunnels or greenhouses, and this may generate habitat isolation if sexual reproduction in the pathogen occurs in nurseries for the tomato-infecting population of *B. cinerea*. Such habitat isolation may contribute to promote adaptation to tomato, by preventing the immigration of alleles which are favorable for infection of non-tomato hosts but not favorable for infection of tomato. Differences in the timing of epidemics are unlikely to contribute to this habitat

599 isolation, as the period of infection of greenhouse tomatoes runs from late to early winter,
600 which includes the period of infection of grape. The same goes for the location of epidemics,
601 since the sites studied were chosen because the two types of crops are grown nearby. A final
602 possibility to explain the lack of gene flow between *B. cinerea* populations from grape and
603 tomato is that the frequency of sexual reproduction might be lower in populations infecting
604 greenhouse tomatoes. Higher winter temperatures and the removal of plant residues in the
605 greenhouse represent conditions that are less conducive to sexual reproduction. However,
606 our estimates of LD decay and recombination rates are not consistent with a substantially
607 lower frequency of sexual reproduction in the population associated with tomato, compared
608 to the population associated with grape.

609 The differences in population structure observed between *B. cinerea* populations from
610 France and California could be due to different cultivation practices. In California, differences
611 in pathogenicity between tomato and other hosts did not lead to genome-wide
612 differentiation, indicating that gene flow occurs between hosts. In France, on the contrary,
613 differences in virulence are associated to genome-wide differentiation, indicating restriction
614 of gene flow. These differences in structure may be explained by the cultivation of tomatoes
615 in open fields in California, which favors dispersal to other crops, while French tomatoes are
616 generally grown in plastic tunnels or greenhouses.

617

618 *Widespread signatures of selection along genomes*

619 We identified little variation in the gene content among T, G1 and G2 populations, with one
620 gene specific to T, 22 genes specific to G1 and five genes shared between G1 and G2 but not
621 T, suggesting that gene gain or loss is not the main process of adaptation to tomato. In

parallel to our analysis of presence/absence variation, our genome scans for positive selection pinpointed several genomic regions which may harbour determinants of ecological differentiation between the population specialized to tomato and the population parasitizing grapevine. In order to cover multiple time scales and different signatures of positive selection, we used a variety of analytical approaches. The McDonald-Kreitman test focuses on genes and detects repeated episodes of selective sweeps fixing non-synonymous substitutions, thus generating a higher ratio of amino acid divergence to polymorphism (Dn / Pn), relative to the ratio of silent divergence to polymorphism (Ds / Ps), than expected under neutrality. The values of nucleotide diversity and Tajima's D measured in the T population specialized in tomatoes were very close to the values measured for the two other populations, which is not consistent with a very recent origin of this population and justifies the use of the McDonald-Kreitman test. Genome scans for selective sweeps detect more recent events, and by nature these methods can also detect genes that are not directly the target of selection, but may have hitch-hiked due to physical linkage with sites under positive selection. However, the LD decay values measured for the T population remain moderate (9kb), and we used a combination of different selective sweep metrics to substantially shorten the list of candidate genes, which should reduce the impact of genetic hitch-hiking on our list of genes under recent positive selection. Despite using a more conservative approach, we identified more selective sweeps than in the generalist *Sclerotinia sclerotiorum* fungus (Derbyshire *et al.* 2019), or in the Californian generalist population of *B. cinerea* (Soltis *et al.* 2019).

644 *Genes under positive selection*

645 We identified a number of genes showing signatures of positive selection using the
646 approaches discussed above and highlighting potential candidates for their role in host
647 specialization. Functional annotation of the *B. cinerea* genome and previous experimental
648 studies provided lists of genes involved in host-pathogen interaction and in other
649 developmental processes (Amselem *et al.* 2011; Nakajima & Akutsu 2014; Rodriguez-
650 Moreno *et al.* 2018). We used these published lists of genes to investigate whether some
651 specific biological processes were subjected to positive selection in the different
652 populations. Our data revealed that the five genes showing the strongest signatures of
653 selection in both the T and G1 populations, but also showing high sequence divergence
654 between the two populations, included two genes encoding for CAZymes with glycoside
655 hydrolase activity, which are potential PCWDEs. We also found that the 428 genes showing
656 the strongest signatures of selection in the T population with McDonald-Kreitman tests were
657 enriched both in genes coding for PCWDEs and in genes coding for enzymes involved in the
658 oxidative stress response. Notably, ten genes encoding secreted CAZymes targeting
659 compounds of the plant cell wall, *i.e.* cellulose and pectin (Amselem et al., 2011; Lombard *et*
660 *al.* 2014), were found under positive selection. One of these ten genes encodes the xylanase
661 BcXyn11A that has previously been shown to be a virulence factor on tomato (Brito *et al.*
662 2006). Another one encodes a cutinase (Bcin01g09430) that was further detected in a
663 selective sweep region suggesting, recurrent and recent positive selection events. Additional
664 PCWDEs were found in other genomic regions identified as selective sweeps. Finally, our
665 comparative genomic analysis suggested that a subtelomeric region that contains two
666 PCWDEs acting on pectin and/or hemicellulose is duplicated in the T population.

667 Necrotrophic species have important repertoires of CAZymes especially those corresponding
668 to PCWDEs which are known to act as major virulence factors in fungi (Zhao *et al.* 2013;
669 Rodriguez-Moreno *et al.* 2018). The genome of the reference isolate of *B. cinerea* (B05.10)
670 revealed 118 PCWDEs (Amselem et al., 2011) and our data suggest that, within this
671 repertoire, some cellulases and pectinases may be of particular importance for the
672 degradation of tomato cell wall. SNPs within a pectinesterase gene were also associated with
673 virulence on tomato in a previous genome-wide association study (Soltis *et al.* 2019).
674 In addition to PCWDEs, the single gene that was present in the T population but missing in
675 the G1 and G2 populations encoded a CAZyme acting on the fungal cell wall, an α-1,3-
676 glucanase classified as a member of the GH71 family. In the fungal cell wall, α-1,3-glucan is a
677 major component that encloses the α-(1,3)-glucan-chitin fibrillar core. Because of its
678 external localization and specific composition, α-1,3-glucan of pathogenic fungi plays a major
679 role in infection-related morphology and host recognition (Beauvais *et al.* 2013; King *et al.*
680 2017). A dozen of genes of *B. cinerea* encode for enzymes of the GH71 family (Amselem et
681 al., 2011). The T-specific GH71 CAZyme might therefore have been retained in the T
682 population as a mean to specifically facilitate infection of tomato by modification of the
683 fungal cell wall resulting in adaptive morphological changes or impairment of host
684 recognition.
685 As mentioned above, the McDonald-Kreitman tests also indicated that eight genes coding
686 for enzymes that detoxify reactive oxygen species showed signatures of positive selection in
687 the T population. During infection, *B. cinerea* encounters an oxidative burst, an early host
688 response that results in the death of plant cells. This mechanism is used in turn by *B. cinerea*
689 to achieve full virulence but this also implies that the fungus has to resist to this toxic

690 environment. The fungal oxidative stress response system includes detoxifying enzymes such
691 as superoxide dismutases (SODs) that convert O_2 into the less toxic H_2O_2, as well as
692 catalases, peroxidases and peroxiredoxins that convert H_2O_2. Additional non-enzymatic
693 mechanisms include the oxidation of compounds such as glutathione (Heller & Tudzynski
694 2011). In addition to the genes encoding SOD (BcSOD3), peroxidases (BcCCP1),
695 peroxiredoxins (BcPRX8) and other detoxifying enzymes sur as glutathione-S-transferases
696 (BcGST1, 9 and 24), a gene encoding the transporter BcAtrO also showed a signature of
697 positive selection in the T population. Inactivation of this gene previously suggested that it
698 allows the efflux of H_2O_2 and resistance this reactive oxygen species (Pane *et al.* 2008).
699 Altogether, our data suggest that the oxidative burst occurring in the *B. cinerea*/tomato
700 interaction is particularly challenging for the fungus.
701
702 *Concluding remarks*
703 We identified a population of *B. cinerea* specialized to tomato, which diverged from a
704 grapevine-associated population. Genome scans for selective sweeps and McDonald-
705 Kreitman tests revealed widespread signatures of positive selection that identified genes
706 that may contribute to the pathogen's adaptation to its tomato host. Candidate genes for
707 specialization to tomato were significantly enriched in those encoding cellulases, pectinases
708 and enzymes involved in the oxidative stress response, suggesting that the ability to degrade
709 the host cell wall and to cope with the oxidative burst are two key process in the *B.*
710 *cinerea*/tomato interaction. Our work sets the stage for future studies aiming to elucidate
711 the phenotypic and fitness effects of the candidate genes for specialization of *B. cinerea* to
712 tomato, for instance by knocking-out or replacing candidate genes for host specialization.

Acknowledgements

AM was supported by a grant from the Doctoral School « Sciences du Végétal », Université Paris-Saclay. We are grateful to INRAE-LIPM Bioinformatics Platform (Jérôme Gouzy, Sébastien Carrère, Erika Sallet, Ludovic Legrand) and Genotoul Bioinformatics Platforms Toulouse Occitanie (Bioinfo Genotoul, doi: 10.15454/1.5572369328961167E12) for providing computational support and resources. This work was supported by a grant overseen by the French National Research Agency (ANR) as part of the "Investissements d'Avenir" Programme (LabEx BASC; ANR-11-LABX-0034) and by the INRAE department SPE. The BIOGER unit also benefits from the support of "Saclay Plant Science-SPS" (ANR-17-EUR-0007).

References

Almagro Armenteros JJ, Tsirigos KD, Sonderby CK, *et al.* (2019) SignalP 5.0 improves signal peptide predictions using deep neural networks. *Nature biotechnology* **37**, 420-423.

Amselem J, Cuomo CA, van Kan JA, *et al.* (2011) Genomic analysis of the necrotrophic fungal pathogens *Sclerotinia sclerotiorum* and *Botrytis cinerea*. *PLoS genetics* **7**, e1002230.

Atwell S, Corwin J, Soltis N, *et al.* (2015) Whole genome resequencing of Botrytis cinerea isolates identifies high levels of standing diversity. *Frontiers in microbiology* **6**, 996.

Atwell S, Corwin JA, Soltis N, *et al.* (2018) Resequencing and association mapping of the generalist pathogen Botrytis cinerea. *bioRxiv*, 489799.

Auton A, McVean G (2007) Recombination rate estimation in the presence of hotspots. *Genome research* **17**, 1219-1227.

Bardin M, Leyronas C, Troulet C, Morris CE (2018) Striking similarities between Botrytis cinerea from non-agricultural and from agricultural habitats. *Frontiers in plant science* **9**, 1820.

Beauvais A, Bozza S, Kniemeyer O, *et al.* (2013) Deletion of the α-(1,3)-glucan synthase genes induces a restructuring of the conidial cell wall responsible for the avirulence of *Aspergillus fumigatus*. *PLoS pathogens* **9**, e1003716.

Bolger AM, Lohse M, Usadel B (2014) Trimmomatic: a flexible trimmer for Illumina sequence data. *Bioinformatics* **30**, 2114-2120.

Bonhomme M, Chevalet C, Servin B, *et al.* (2010) Detecting selection in population trees: the Lewontin and Krakauer test extended. *Genetics* **186**, 241-262.

Brito N, Espino JJ, González C (2006) The endo-β-1, 4-xylanase Xyn11A is required for virulence in Botrytis cinerea. *Molecular Plant-Microbe Interactions* **19**, 25-32.

Caseys C, Shi G, Soltis N, *et al.* (2020) Quantitative interactions drive *Botrytis cinerea* disease outcome across the plant kingdom. *bioRxiv*, 507491.

Cummings CA, Brinig MM, Lepp PW, van de Pas S, Relman DA (2004) Bordetella species are distinguished by patterns of substantial gene loss and host adaptation. *Journal of bacteriology* **186**, 1484-1492.

Decognet V, Bardin M, Trottin-Caudal Y, Nicot PC (2009) Rapid change in the genetic diversity of *Botrytis cinerea* populations after the introduction of strains in a tomato glasshouse. *Phytopathology* **99**, 185-193.

Dellaporta SL, Wood J, Hicks JB (1983) A plant DNA minipreparation: Version II. *Plant Molecular Biology Reporter* **1**, 19-21.

Derbyshire MC, Denton-Giles M, Hane JK, *et al.* (2019) A whole genome scan of SNP data suggests a lack of abundant hard selective sweeps in the genome of the broad host range plant pathogenic fungus Sclerotinia sclerotiorum. *PloS one* **14**, e0214201.

759 Elad Y, Pertot I, Prado AMC, Stewart A (2016) Plant hosts of Botrytis spp. In: *Botrytis–the fungus, the pathogen*
760 *and its management in agricultural systems*, pp. 413-486. Springer.
761 Emms DM, Kelly S (2015) OrthoFinder: solving fundamental biases in whole genome comparisons dramatically
762 improves orthogroup inference accuracy. *Genome biology* **16**, 157.
763 Espino JJ, Gutierrez-Sanchez G, Brito N, *et al.* (2010) The *Botrytis cinerea* early secretome. *Proteomics* **10**, 3020-
764 3034.
765 Fariello MI, Boitard S, Naya H, SanCristobal M, Servin B (2013) Detecting signatures of selection through
766 haplotype differentiation among hierarchically structured populations. *Genetics* **193**, 929-941.
767 Ferrer-Admetlla A, Liang M, Korneliussen T, Nielsen R (2014) On detecting incomplete soft or hard selective
768 sweeps using haplotype structure. *Molecular biology and evolution* **31**, 1275-1291.
769 Fisher MC, Henk DlA, Briggs CJ, *et al.* (2012) Emerging fungal threats to animal, plant and ecosystem health.
770 *Nature* **484**, 186.
771 Fournier E, Giraud T (2008) Sympatric genetic differentiation of a generalist pathogenic fungus, *Botrytis cinerea*,
772 on two different host plants, grapevine and bramble. *Journal of Evolutionary Biology* **21**, 122-132.
773 Garrison E, Marth G (2012) Haplotype-based variant detection from short-read sequencing. *arXiv:1207.3907 [q-*
774 *bio]*.
775 Geib E, Markus Gressler M, Iuliia Viediernikova I, Falk Hillmann F, Ilse D. Jacobsen ID, Sandor Nietzsche S,
776 Christian Hertweck C, Matthias Brock M (2016) A Non-canonical Melanin Biosynthesis Pathway
777 Protects Aspergillus terreus Conidia from Environmental Stress. *Cell Chemical Biology* **23**, 587-597.
778 Giraud T (2006) Speciation: Selection against migrant pathogens: the immigrant inviability barrier in pathogens.
779 *Heredity* **97**, 316-318.
780 Giraud T, Gladieux P, Gavrilets S (2010) Linking the emergence of fungal plant diseases with ecological
781 speciation. *Trends in ecology & evolution* **25**, 387-395.
782 Giraud T, Refrégier G, Le Gac M, de Vienne DM, Hood ME (2008) Speciation in fungi. *Fungal genetics and*
783 *biology : FG & B* **45**, 791-802.
784 Gladieux P, Guerin F, Giraud T, *et al.* (2011) Emergence of novel fungal pathogens by ecological speciation:
785 importance of the reduced viability of immigrants. *Molecular ecology* **20**, 4521-4532.
786 Gladieux P, Ravel S, Rieux A, *et al.* (2018) Coexistence of multiple endemic and pandemic lineages of the rice
787 blast pathogen. *MBio* **9**.
788 Gutenkunst RN, Hernandez RD, Williamson SH, Bustamante CD (2009) Inferring the joint demographic history
789 of multiple populations from multidimensional SNP frequency data. *PLoS genetics* **5**, e1000695.
790 Hartmann FE, McDonald BA, Croll D (2018) Genome-wide evidence for divergent selection between
791 populations of a major agricultural pathogen. *Molecular ecology* **27**, 2725-2741.
792 Heller J, Tudzynski P (2011) Reactive oxygen species in phytopathogenic fungi: signaling, development, and
793 disease. *Annual review of phytopathology* **49**, 369-390.
794 Huson DH, Bryant D (2005) Estimating phylogenetic trees and networks using SplitsTree 4. *Manuscript in*
795 *preparation, software available from www. splitstree. org*.

796 Inoue Y, Vy TTP, Yoshida K, *et al.* (2017) Evolution of the wheat blast fungus through functional losses in a host
797 specificity determinant. *Science* **357**, 80-83.
798 Johnson M, Zaretskaya I, Raytselis Y, *et al.* (2008) NCBI BLAST: a better web interface. *Nucleic acids research* **36**,
799 W5-W9.
800 Jones P, Binns D, Chang HY, *et al.* (2014) InterProScan 5: genome-scale protein function classification.
801 *Bioinformatics* **30**, 1236-1240.
802 Khvorykh GV, Khrunin AV (2020) imputeqc: an R package for assessing imputation quality of genotypes and
803 optimizing imputation parameters. *BMC bioinformatics* **21**, 1-14.
804 King R, Urban M, Lauder RP, *et al.* (2017) A conserved fungal glycosyltransferase facilitates pathogenesis of
805 plants by enabling hyphal growth on solid surfaces. *PLoS pathogens* **13**, e1006672.
806 Krogh A, Larsson B, Von Heijne G, Sonnhammer ELL (2001) Predicting transmembrane protein topology with a
807 hidden Markov model: application to complete genomes. *Journal of molecular biology* **305**, 567-580.
808 Langridge GC, Fookes M, Connor TR, *et al.* (2015) Patterns of genome evolution that have accompanied host
809 adaptation in *Salmonella*. *Proceedings of the National Academy of Sciences of the United States of*
810 *America* **112**, 863-868.
811 Leyronas C, Bardin M, Berthier K, *et al.* (2018) Assessing the phenotypic and genotypic diversity of *Sclerotinia*
812 *sclerotiorum* in France. *European journal of plant pathology* **152**, 933-944.
813 Li H (2014) Toward better understanding of artifacts in variant calling from high-coverage samples.
814 *Bioinformatics (Oxford, England)* **30**, 2843-2851.
815 Li H, Durbin R (2009) Fast and accurate short read alignment with Burrows-Wheeler transform. *Bioinformatics*
816 **25**, 1754-1760.
817 Li H, Handsaker B, Wysoker A, *et al.* (2009) The Sequence Alignment/Map format and SAMtools. *Bioinformatics*
818 **25**, 2078-2079.
819 Lombard V, Golaconda Ramulu H, Drula E, Coutinho PM, Henrissat B (2014) The Carbohydrate-Active enZymes
820 database (CAZy) in 2013. *Nucleic acids research* **42**, D490-495.
821 Luo R, Liu B, Xie Y, *et al.* (2012) SOAPdenovo2: an empirically improved memory-efficient short-read de novo
822 assembler. *GigaScience* **1**, 18.
823 Ma Z, Michailides TJ (2005) Genetic structure of Botrytis cinerea populations from different host plants in
824 California. *Plant disease* **89**, 1083-1089.
825 Marchi N, Excoffier L (2020) Gene flow as a simple cause for an excess of high-frequency-derived alleles.
826 *Evolutionary applications* **13**, 2254-2263.
827 Maruthachalam K, Klosterman SJ, Kang S, Hayes RJ, Subbarao KV (2011) Identification of pathogenicity-related
828 genes in the vascular wilt fungus *Verticillium dahliae* by *Agrobacterium tumefaciens*-mediated T-DNA
829 insertional mutagenesis. *Molecular Biotechnology* **49**, 209-221.
830 McCarthy DJ, Chen Y, Smyth GK (2012) Differential expression analysis of multifactor RNA-Seq experiments
831 with respect to biological variation. *Nucleic acids research* **40**, 4288-4297.

McDonald JH, Kreitman M (1991) Adaptive protein evolution at the Adh locus in *Drosophila*. *Nature* **351**, 652-654.

Mercier A, Carpentier F, Duplaix C, *et al.* (2019) The polyphagous plant pathogenic fungus *Botrytis cinerea* encompasses host-specialized and generalist populations. *Environmental microbiology*.

Nakajima M, Akutsu K (2014) Virulence factors of *Botrytis cinerea*. *Journal of General Plant Pathology* **80**, 15-23.

Nielsen R, Beaumont MA (2009) Statistical inferences in phylogeography. *Molecular ecology* **18**, 1034-1047.

Nielsen R, Williamson S, Kim Y, *et al.* (2005) Genomic scans for selective sweeps using SNP data. *Genome research* **15**, 1566-1575.

Nosil P, Vines TH, Funk DJ (2005) Perspective: reproductive isolation caused by natural selection against immigrants from divergent habitats. *Evolution; international journal of organic evolution* **59**, 705-719.

Pane C, Rekab D, Firrao G, Ruocco M, Scala F (2008) A NOVEL GENE CODING FOR AN ABC TRANSPORTER IN BOTRYTIS CINEREA (BOTRYOTINIA FUCKELIANA) IS INVOLVED IN RESISTANCE TO H^+ O^+. *Journal of Plant Pathology*, 453-462.

Pavlidis P, Zivkovic D, Stamatakis A, Alachiotis N (2013) SweeD: likelihood-based detection of selective sweeps in thousands of genomes. *Molecular biology and evolution* **30**, 2224-2234.

Perlin MH, Andrews J, Toh SS (2014) Essential letters in the fungal alphabet: ABC and MFS transporters and their roles in survival and pathogenicity. *Advances in genetics* **85**, 201-253.

Plaza V, Lagües Y, Carvajal M, *et al.* (2015) bcpmr1 encodes a P-type Ca2+/Mn2+-ATPase mediating cell-wall integrity and virulence in the phytopathogen Botrytis cinerea. *Fungal Genetics and Biology* **76**, 36-46.

Porquier A, Morgant G, Moraga J, *et al.* (2016) The botrydial biosynthetic gene cluster of *Botrytis cinerea* displays a bipartite genomic structure and is positively regulated by the putative Zn(II)2Cys6 transcription factor BcBot6. *Fungal genetics and biology : FG & B* **96**, 33-46.

Reich D, Thangaraj K, Patterson N, Price AL, Singh L (2009) Reconstructing Indian population history. *Nature* **461**, 489-494.

Robinson MD, McCarthy DJ, Smyth GK (2010) edgeR: a Bioconductor package for differential expression analysis of digital gene expression data. *Bioinformatics (Oxford, England)* **26**, 139-140.

Rodriguez-Moreno L, Ebert MK, Bolton MD, Thomma BPHJ (2018) Tools of the crook- infection strategies of fungal plant pathogens. *The Plant journal : for cell and molecular biology* **93**, 664-674.

Rosebeck S, Leaman DW (2008) Mitochondrial localization and pro-apoptotic effects of the interferon-inducible protein ISG12a. *Apoptosis : an international journal on programmed cell death* **13**, 562-572.

Scheet P, Stephens M (2006) A fast and flexible statistical model for large-scale population genotype data: applications to inferring missing genotypes and haplotypic phase. *The American Journal of Human Genetics* **78**, 629-644.

Schulze-Lefert P, Panstruga R (2011) A molecular evolutionary concept connecting nonhost resistance, pathogen host range, and pathogen speciation. *Trends in plant science* **16**, 117-125.

Seppey M, Manni M, Zdobnov EM (2019) BUSCO: assessing genome assembly and annotation completeness. In: *Gene Prediction*, pp. 227-245. Springer.

869 Servedio MR, Van Doorn GS, Kopp M, Frame AM, Nosil P (2011) Magic traits in speciation: 'magic' but not rare?
870 *Trends in ecology & evolution* **26**, 389-397.
871 Simko I, Piepho H-P (2012) The area under the disease progress stairs: calculation, advantage, and application.
872 *Phytopathology* **102**, 381-389.
873 Skoglund P, Mallick S, Bortolini MC, *et al.* (2015) Genetic evidence for two founding populations of the
874 Americas. *Nature* **525**, 104-108.
875 Solovyev V, Kosarev P, Seledsov I, Vorobyev D (2006) Automatic annotation of eukaryotic genes, pseudogenes
876 and promoters. *Genome biology* **7**, S10.11-12.
877 Soltis NE, Atwell S, Shi G, *et al.* (2019) Interactions of tomato and Botrytis cinerea genetic diversity: Parsing the
878 contributions of host differentiation, domestication, and pathogen variation. *The Plant Cell* **31**, 502-
879 519.
880 Sonnhammer ELL, Von Heijne G, Krogh A A hidden Markov model for predicting transmembrane helices in
881 protein sequences **6**, 175-182.
882 Stoletzki N, Eyre-Walker A (2011) Estimation of the neutrality index. *Molecular biology and evolution* **28**, 63-70.
883 Stukenbrock EH, McDonald BA (2008) The origins of plant pathogens in agro-ecosystems. *Annual review of*
884 *phytopathology* **46**, 75-100.
885 Szpiech ZA, Jakobsson M, Rosenberg NA (2008) ADZE: a rarefaction approach for counting alleles private to
886 combinations of populations. *Bioinformatics (Oxford, England)* **24**, 2498-2504.
887 Valette-Collet O, Cimerman A, Reignault P, Levis C, Boccara M (2003) Disruption of Botrytis cinerea pectin
888 methylesterase gene Bcpme1 reduces virulence on several host plants. *Molecular Plant-Microbe*
889 *Interactions* **16**, 360-367.
890 van Kan JA, Stassen JH, Mosbach A, *et al.* (2017) A gapless genome sequence of the fungus *Botrytis cinerea*.
891 *Molecular plant pathology* **18**, 75-89.
892 Walker A (2016) Diversity within and between species of *Botrytis*. In: *Botrytis - The Fungus, the Pathogen and*
893 *its Management in Agricultural Systems* (eds. Fillinger S, Elad Y), pp. 91-125.
894 Walker A, Gladieux P, Decognet V, *et al.* (2015) Population structure and temporal maintenance of the
895 multihost fungal pathogen *Botrytis cinerea*: causes and implications for disease management.
896 *Environmental microbiology* **17**, 1261-1274.
897 Yang Z (1997) PAML: a program package for phylogenetic analysis by maximum likelihood. *Computer*
898 *applications in the biosciences* **13**, 555-556.
899 Yang Z (2007) PAML 4: phylogenetic analysis by maximum likelihood. *Molecular biology and evolution* **24**, 1586-
900 1591.
901 Zerbino DR, Birney E (2008) Velvet: algorithms for de novo short read assembly using de Bruijn graphs. *Genome*
902 *research* **18**, 821-829.
903 Zhang C, Dong SS, Xu JY, He WM, Yang TL (2019a) PopLDdecay: a fast and effective tool for linkage
904 disequilibrium decay analysis based on variant call format files. *Bioinformatics (Oxford, England)* **35**,
905 1786-1788.

Zhang C, Dong SS, Xu JY, He WM, Yang TL (2019b) PopLDdecay: a fast and effective tool for linkage disequilibrium decay analysis based on variant call format files. *Bioinformatics* **35**, 1786-1788.

Zhang MZ, Sun CH, Liu Y, *et al.* (2020) Transcriptome analysis and functional validation reveal a novel gene, BcCGF1, that enhances fungal virulence by promoting infection-related development and host penetration. *Molecular plant pathology* **21**, 834-853.

Zhao Z, Liu H, Wang C, Xu JR (2013) Comparative analysis of fungal genomes reveals different plant cell wall degrading capacity in fungi. *BMC genomics* **14**, 274.

Zhong Z, Marcel TC, Hartmann FE, *et al.* (2017) A small secreted protein in *Zymoseptoria tritici* is responsible for avirulence on wheat cultivars carrying the Stb6 resistance gene. *The New phytologist* **214**, 619-631.

Table 1. *Botrytis* isolates included in the study. Isolates from grapevine berries and tomatoes were collected in three regions of France between September 2005 and June 2007 for Champagne and Provence isolates (Walker *et al.* (2015), and between May and June 2009 for Occitanie isolates. Tomatoes in Occitanie were grown in plastic tunnels with sides open, whereas those from the Champagne and Provence areas were grown in glass-greenhouses. B05.10 is used as the reference isolate for genomic analysis (van Kan et al. 2016)

Species	Isolate ID	Other ID	Host, cultivar	Region, city
B. cinerea	Vv1	VC636	*Vitis vinifera,* Pinot noir	Champagne, Hautvilliers
	Vv2	VC095	*Vitis vinifera,* Pinot noir	Champagne, Vandières
	Vv3	VC621	*Vitis vinifera,* Pinot noir	Champagne, Hautvilliers
	Vv4	VC671	*Vitis vinifera,* Pinot noir	Champagne, Hautvilliers
	Vv5	VC224	*Vitis vinifera,* Pinot meunier	Champagne, Courteron
	Vv6	VC624	*Vitis vinifera,* Pinot noir	Champagne, Hautvilliers
	Vv7	ACBER342	*Vitis vinifera,* Grenache	Provence, Berre
	Vv8	ACBER356	*Vitis vinifera,* Grenache	Provence, Berre
	Vv9	ACBER358	*Vitis vinifera,* Grenache	Provence, Berre
	Vv10	ACSAR333	*Vitis vinifera,* Grenache	Provence, Sarrians
	Vv11	ACSAR334	*Vitis vinifera,* Grenache	Provence, Sarrians
	Vv12	ACSAR335	*Vitis vinifera,* Grenache	Provence, Sarrians
	Vv13	ACSAR342	*Vitis vinifera,* Grenache	Provence, Sarrians
	Vv14	ACSAR354	*Vitis vinifera,* Grenache	Provence, Sarrians
	Vv15	ACSAR357	*Vitis vinifera,* Grenache	Provence, Sarrians
	Vv16	VC610	*Vitis vinifera,* Pinot noir	Champagne, Hautvilliers
	Sl1	VA714	*Solanum lycopersicum,* Moneymaker	Champagne, Foissy-sur-Vanne
	Sl2	VC800	*Solanum lycopersicum,* Moneymaker	Champagne, Courceroy
	Sl3	VC806	*Solanum lycopersicum,* Moneymaker	Champagne, Courceroy
	Sl4	AABER19	*Solanum lycopersicum*, Alison	Provence, Berre
	Sl5	ACBER304	*Solanum lycopersicum*, Alison	Provence, Berre
	Sl6	ACPIE306	*Solanum lycopersicum,* Hipop	Provence, Pierrelatte
	Sl7	ADPIE463	*Solanum lycopersicum,* Hipop	Provence, Pierrelatte
	Sl8	ADPIE475	*Solanum lycopersicum,* Hipop	Provence, Pierrelatte
	Sl9	65_TT8	*Solanum lycopersicum*, Brenda	Occitanie, Alenya
	Sl10	5_TT8	*Solanum lycopersicum*, Brenda	Occitanie, Alenya
	Sl11	13_TT8	*Solanum lycopersicum*, Brenda	Occitanie, Alenya

	Sl12	9_TT8	*Solanum lycopersicum*, Brenda	Occitanie, Alenya
	Sl13	66_TT8	*Solanum lycopersicum*, Brenda	Occitanie, Alenya
	Rf1	VC902	*Rubus fruticosus*, wild	Champagne, Foissy-sur-Vanne
	Rf2	VC399	*Rubus fruticosus*, wild	Champagne, Courteron
	Hm1	MSN-Bot 2556	*Hydrangea macrophylla*, Leuchtfeuer	Anjou, Angers
	B05.10	-	-	-
B. fabae	Bfab	MSN-Bot 2220	*Vicia faba*	Region of Tunis (Tunisia)

Table 2. Summary statistics of genomic variation in three clusters of *Botrytis cinerea*

Cluster	S	π	θ	AR	PAR	D	H	LD50	ρ
T	37763	0.0027	0.0026	1.094 (0.0002)	0.073 (0.0002)	0.309	0.451	8600	0.0108
G1	26769	0.0018	0.0017	1.078 (0.0002)	0.085 (0.0002)	0.167	0.230	3100	0.0178
G2	14307	0.0030	0.0027	1.104 (0.0003)	0.071 (0.0002)	1.470	0.140	16800	0.2047

S, number of segregating sites; π, nucleotide diversity per site; θ, Watterson's estimate of the population mutation parameter per site; ρ, population recombination parameter per site; AR, allelic richness (standard error of the mean); PAR, private allele richness (standard error of the mean); D, Tajima's D; H, Fay and Wu's standardised H; LD50, distance (in bp) at which linkage disequilibrium reaches half of its maximum value. Only core chromosomes BCIN01 to BCIN16 were included in calculations. Per site estimates of π, ρ and θ were computed by summing across chromosomes and dividing by number of sites covered. Tajima's D and Fay and Wu's standardised H were computed across 10kb windows, and averaged. AR and PAR were computed using a generalized rarefaction approach and a standardized sample size of two haploid genomes.

Figure Captions

Figure 1. Population subdivision inferred based on SNPs identified in 32 isolates of *Botrytis cinerea* collected on tomato (red, Sl prefix, *Solanum lycopersicum*), grape (green, Vv prefix, *Vitis vinifera*), bramble (black, Rf prefix, *Rubus fruticosus*) and hydrangea (black, Hm prefix, *Hydrangea macrophylla*). (A) Ancestry proportions in K clusters, as estimated with the sNMF program. Each multilocus genotype is represented by a vertical bar divided into K segments, indicating membership in K clusters. (B) Neighbor-net phylogenetic network estimated with SPLITSTREE, with one isolate of *B. fabae* (Bfab) used as the outgroup. Reticulations indicate phylogenetic conflicts caused by recombination or incomplete lineage sorting. (C) Principal component analysis showing first four principal components PC1, PC2, PC3 and PC4. Isolate B05.10 in (A) and (B) is the reference genome for *B. cinerea* (van Kan et al. 2016)

Figure 2. Site frequency spectra estimated in populations T2 and Vv1 based on 85,415 SNPs using the python package DADI, projecting sample sizes to seven haploid genomes. Projection consists in averaging over all possible re-samplings of the larger sample size data, thus biallelic positions with data for less than seven individuals are not included in calculations and not counted as SNPs.

Figure 3. Boxplots representing the extent of aggressiveness (% relative to the reference isolate BC1) on tomato of the *Botrytis cinerea* isolates collected on grapevine (n=16) and tomato (n=13). For each boxplot, mean (crosses), median (horizontal lines), values of the aggressiveness index (circles), 25-75% quartiles, and maximum and minimum values are represented.

Figure 4. Genome scans for selective sweeps in the T and G1 populations of *Botrytis cinerea*, parasitizing tomato and grapevine, respectively. (A) and (C): Composite likelihood ratio

(CLR) estimated using the SWEED software (Nielsen *et al.* 2005; Pavlidis *et al.*, 2013) in T and G1, respectively. (B) and (D) Number of segregating sites by length, nS_L, estimated using the NSL software (Ferrer-Admetlla *et al.* 2014) in T and G1, respectively. (E) hapFLK statistic estimated using the HAPFLK software (Bonhomme *et al.* 2010; Fariello *et al.* 2013). Horizontal dashed black lines represent the top 5%. Vertical dashed grey lines represent the boundaries of the 16 chromosomes and the chromosome names are set along the x axis. SNPs in chromosomes with names ending with odd numbers are represented in dark colors, while SNPs in chromosomes with names ending with even numbers are represented in light colors. Black dots represent SNPs belonging to the following set: [(top 5% CLR population G1) ∪ (top 5% CLR population T) ∪ (top 5% nSL population G1) ∪ (top 5% nSL population T)] ∩ [top 5% hapFLK].

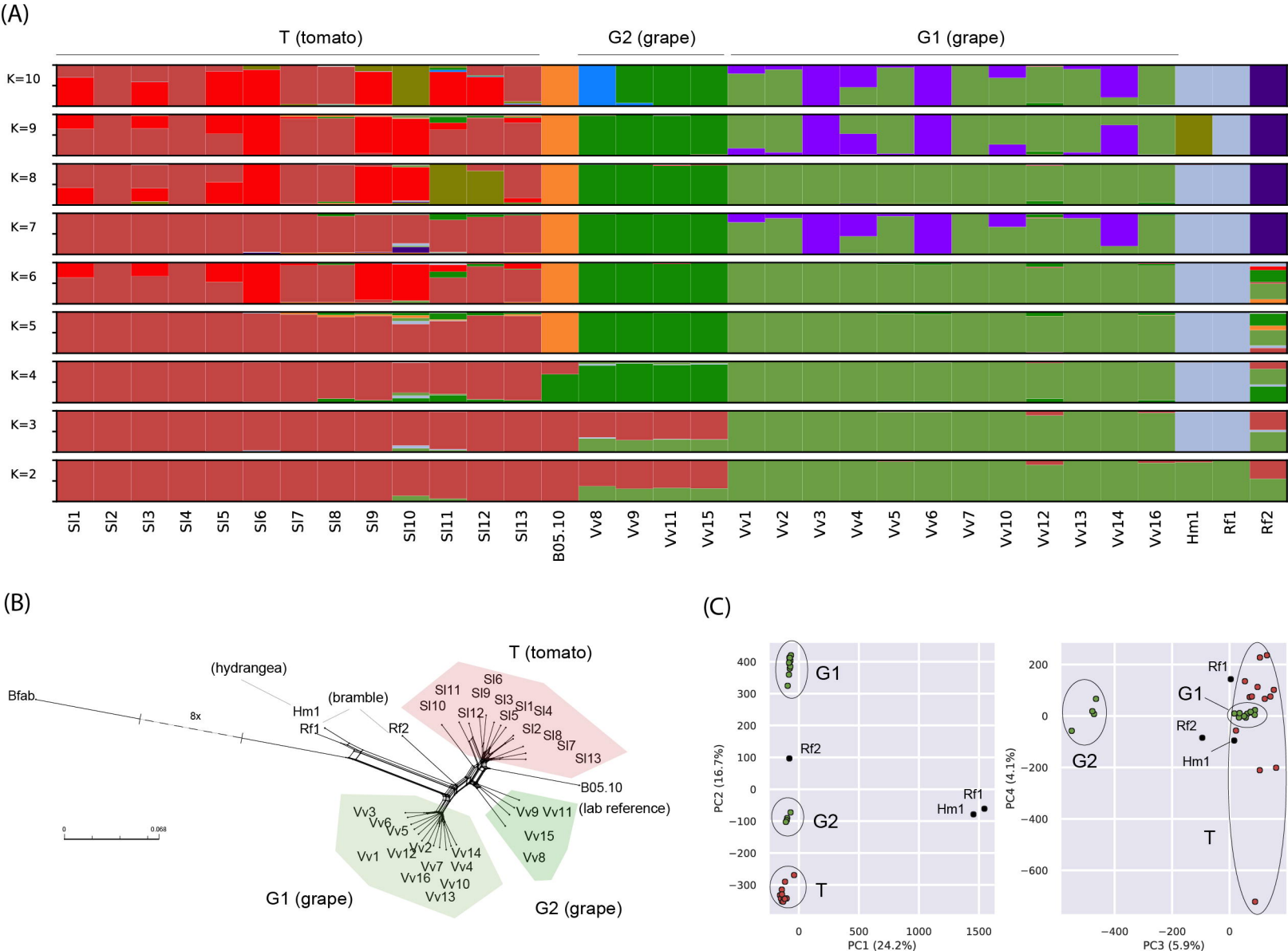
(A)
T (tomato)
G2 (grape)
G1 (grape)
K=10
K=9
K=8
K=7
K=6
K=5
K=4
K=3
K=2
Sl1 Sl2 Sl3 Sl4 Sl5 Sl6 Sl7 Sl8 Sl9 Sl10 Sl11 Sl12 Sl13 B05.10 Vv8 Vv9 Vv11 Vv15 Vv1 Vv2 Vv3 Vv4 Vv5 Vv6 Vv7 Vv10 Vv12 Vv13 Vv14 Vv16 Hm1 Rf1 Rf2
(B)
Bfab
8x
(hydrangea)
(bramble)
Hm1
Rf1
Rf2
T (tomato)
Sl6 Sl11 Sl9 Sl3 Sl1 Sl4 Sl10 Sl12 Sl5 Sl2 Sl8 Sl7 Sl13
B05.10
(lab reference)
Vv9 Vv11
Vv15
Vv8
Vv3 Vv6 Vv5 Vv2 Vv1 Vv12 Vv14 Vv7 Vv4 Vv16 Vv10 Vv13
G1 (grape)
G2 (grape)
0
0.068
(C)
G1
G2
T
Rf2
Rf1
Hm1
PC2 (16.7%)
PC1 (24.2%)
PC4 (4.1%)
PC3 (5.9%)

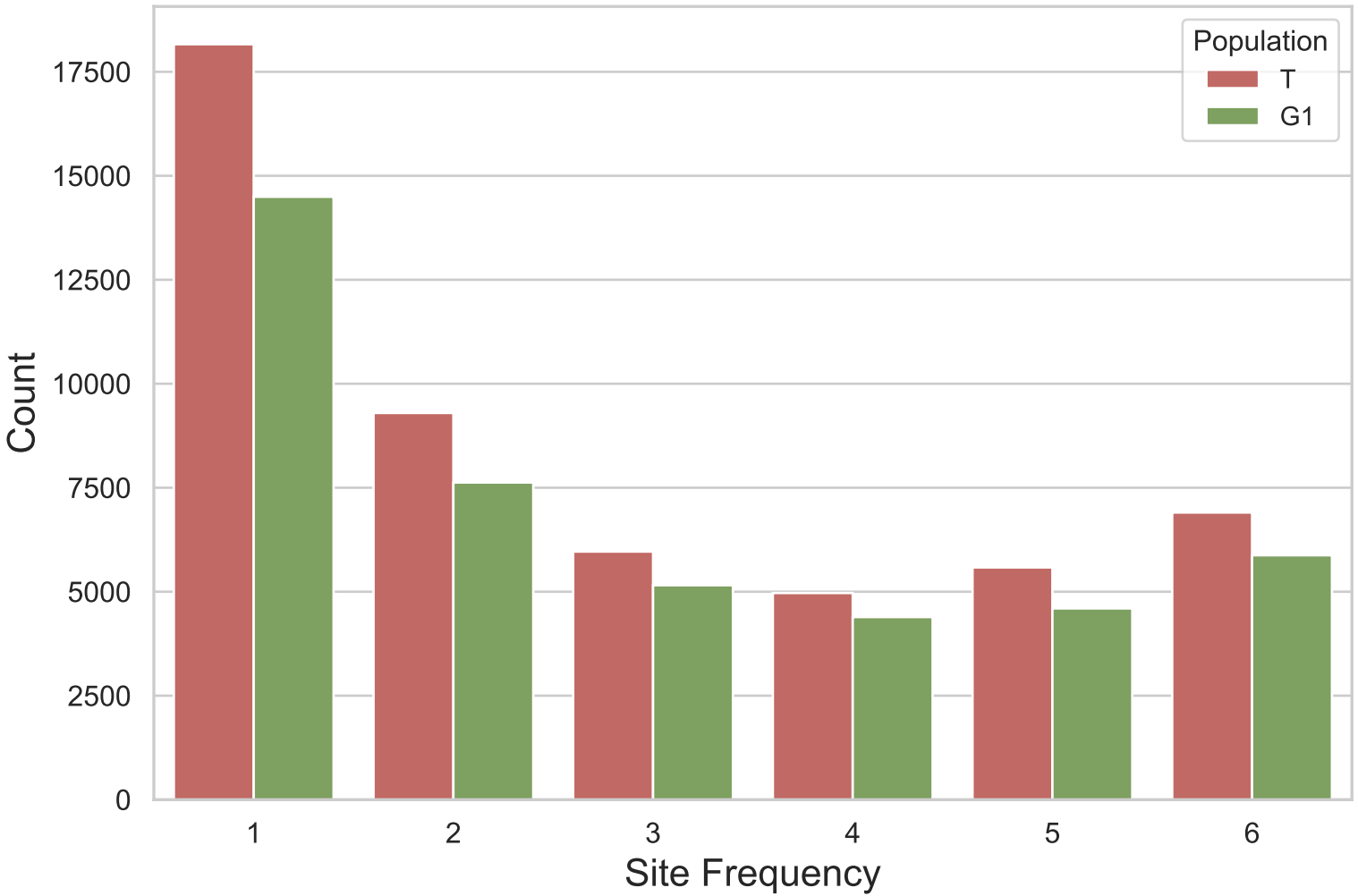
Population
T
G1
17500
15000
12500
10000
7500
5000
2500
0
Count
1
2
3
4
5
6
Site Frequency

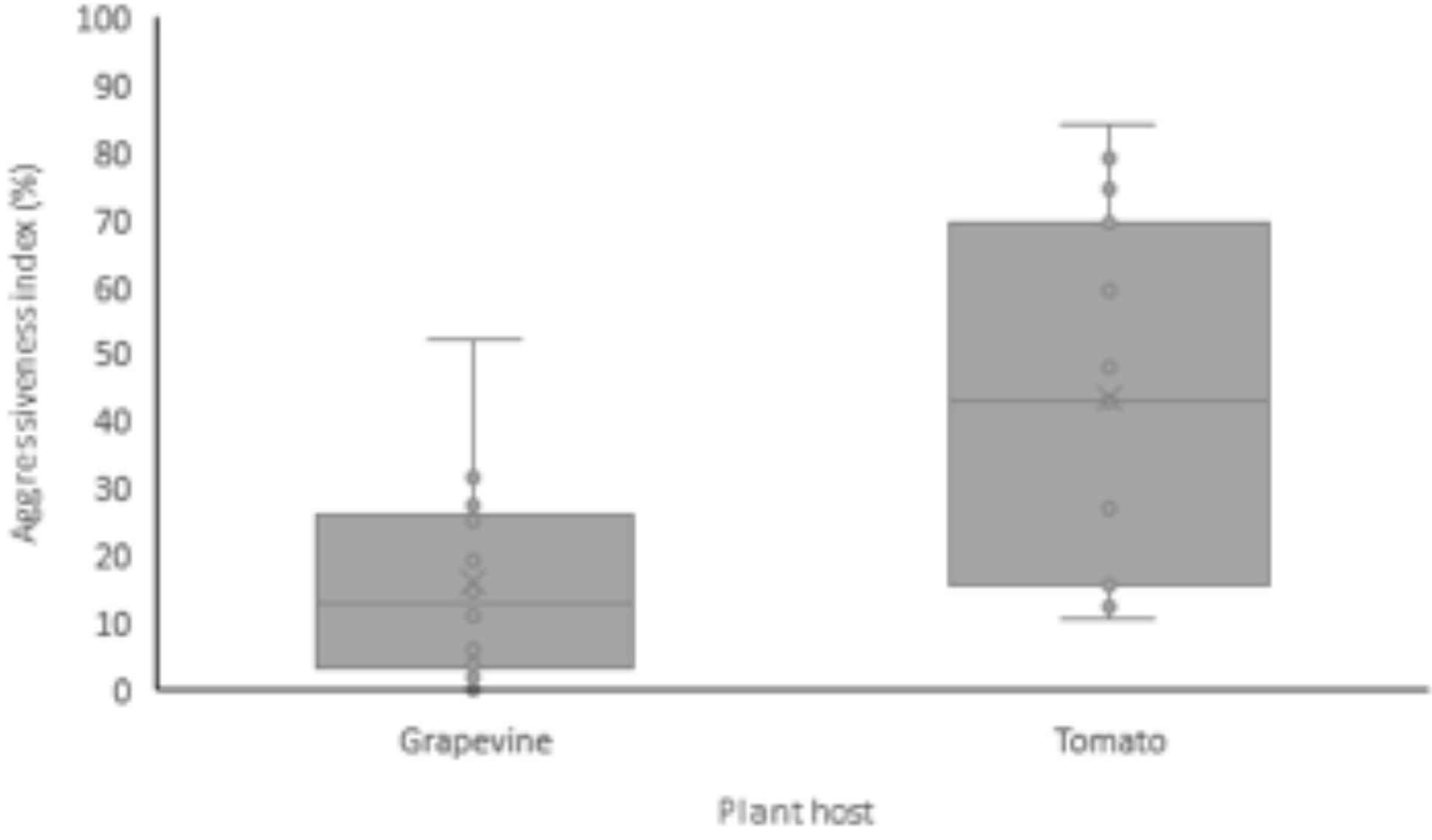
100
90
80
70
60
50
40
30
20
10
0
Aggressiveness index (%)
Grapevine
Tomato
Plant host

(A) population T

(B) population T

(C) population G1

(D) population G1

(E) population T vs population G1

BCIN01 BCIN02 BCIN03 BCIN04 BCIN05 BCIN06 BCIN07 BCIN08 BCIN09 BCIN10 BCIN11 BCIN12 BCIN13 BCIN14 BCIN15 BCIN16